# Plant Physiology®

# HISTONE DEACETYLASE 6 suppresses salicylic acid biosynthesis to repress autoimmunity

Zhenjiang Wu [1], Lei He,[1] Ye Jin,[1] Jing Chen,[1] Huazhong Shi [1,2] Yizhong Wang [1,*,†] and Wannian Yang [1,†]

1 School of Life Sciences, Central China Normal University, Wuhan, 43009 Hubei, PR China
2 Department of Chemistry and Biochemistry, Texas Tech University, Lubbock, Texas 79409, USA

*Author for communication: wyzhong@mail.ccnu.edu.cn
†Senior author.
These authors contributed equally (Z.W., L.H., Y.J.).
Z.W. L.H. Y.J., and J.C. performed the experiments. W.Y. and Y.W. conceived and designed the experiments. Y.W. wrote the manuscript, H.S. and W.Y. revised it.
The author responsible for distribution of materials integral to the findings presented in this article in accordance with the policy described in the Instructions for Authors (https://academic.oup.com/plphys/pages/general-instructions) is: Yizhong Wang (wyzhong@mail.ccnu.edu.cn)

## Abstract

Salicylic acid (SA) plays an important role for plant immunity, especially resistance against biotrophic pathogens. SA quickly accumulates after pathogen attack to activate downstream immunity events and is normally associated with a tradeoff in plant growth. Therefore, the SA level in plants has to be strictly controlled when pathogens are absent, but how this occurs is not well understood. Previously we found that in Arabidopsis (*Arabidopsis thaliana*), HISTONE DEACETYLASE 6 (HDA6), a negative regulator of gene expression, plays an essential role in plant immunity since its mutation allele *shining 5* (*shi5*) exhibits autoimmune phenotypes. Here we report that this role is mainly through suppression of SA biosynthesis: first, the autoimmune phenotypes and higher resistance to *Pst* DC3000 of *shi5* mutants depended on SA; second, SA significantly accumulated in *shi5* mutants; third, HDA6 repressed SA biosynthesis by directly controlling the expression of *CALMODULIN BINDING PROTEIN 60g* (*CBP60g*) and *SYSTEMIC ACQUIRED RESISTANCE DEFICIENT 1* (*SARD1*). HDA6 bound to the chromatin of *CBP60g* and *SARD1* promoter regions, and histone H3 acetylation was highly enriched within these regions. Furthermore, the transcriptome of *shi5* mutants mimicked that of plants treated with exogenous SA or attacked by pathogens. All these data suggest that HDA6 is vital for plants in finely controlling the SA level to regulate plant immunity.

## Introduction

Being sessile organisms, plants could not avoid unfavorable environments such as abiotic and biotic stresses intentionally. Salicylic acid (SA), as one major plant hormone, is vital for plants to respond to such adverse conditions, especially when facing pathogens (Jones and Dangl, 2006; Rivas-San Vicente and Plasencia, 2011; van Butselaar and Van den Ackerveken, 2020). The important role of SA was well characterized in defense response (Kumar, 2014). Generally, SA is considered to work effectively in the resistance against biotrophic and hemi-biotrophic pathogens. Furthermore, SA is essential for all three layers of immunity, from local pathogen-associated molecular pattern (PAMP)-triggered immunity and effector-triggered immunity to distal systemic-acquired resistance (SAR) (Tsuda et al., 2008; Fu and Dong, 2013; Kachroo et al., 2020).

In Arabidopsis (*Arabidopsis thaliana*), SA is synthesized mainly through two different pathways: the phenylalanine ammonia-lyase (PAL) pathway and the isochorismate (IC) pathway, although both pathways originate from the same substrate chorismate (CA) (Dempsey et al., 2011). The fast accumulation of SA after pathogen attack depends on the IC pathway, in which CA is converted to IC by ISOCHORISMATE SYNTHASE 1 (ICS1) in the plastids (Dempsey et al., 2011). The attenuation of *ICS1* expression in *ics1* mutants causes dramatically reduced SA formation after pathogen infection compared to wild-type (WT) plants, implying the essential role of *ICS1* in SA biosynthesis during pathogen response (Wildermuth et al., 2001). IC is transported to the cytosol by chloroplast envelope located ENHANCED DISEASE SUSCEPTIBILITY 5 (EDS5) (Serrano et al., 2013), at where it is catalyzed to SA through isochorismoyl-9-glutamate (IC-9-Glu) by PBS3/GH3.12, an isochorismoyl-glutamate synthase (Rekhter et al., 2019). IC-9-Glu could spontaneously breakdown into SA, which is enhanced by ENHANCED PSEUDOMONAS SUSCEPTIBILTY 1, a BAHD acyltransferase-like protein, and act as an IC-9-Glu pyruvoyl-glutamate lyase (Huang et al., 2020).

For the SA signal transduction, NONEXPRESSER OF PR GENES 1 (NPR1), which contains ankyrin repeat domains, plays a central role (Lu, 2009). Accumulated SA alters the cellular redox status resulting in the nuclear translocation of NPR1 (Mou et al., 2003). Furthermore, SA mediates NPR1 post-translational modification to regulate the stability of NPR1 protein and its turnover (Spoel et al., 2009; Fu et al., 2012; Withers and Dong, 2017). Recent studies suggest NPR1 acts as a SA receptor as well as NPR3/4, and that the binding of SA to these receptors could change their conformations to turn on the activation activity of NPR1 and turn off the repression activity of NPR3/4, then activate the downstream reactions such as pathogenesis-related (*PR*) genes induction and pathogen resistance (Ding et al., 2018; Ding and Ding, 2020). However, in the tissues where pathogen infection occurs, a rapid rise of SA concentration could cause NPR1 degradation thus inducing the localized hypersensitive response (HR) which shows a necrotic phenotype (Hofius et al., 2009; Minina et al., 2014).

Thus, the biosynthesis of SA has to be tightly regulated to ensure an effective but not excessive response upon pathogen infection. EDS1 and PHYTOALEXIN-DEFICIENT 4 (PAD4) could act together to activate SA synthesis (Feys et al., 2001). Their mutants show reduced SA levels compared to WT and are susceptible to *Pseudomonas syringae* pv. *maculicola* strain ES4326 (*Pma* ES4326) (Venugopal et al., 2009; Cui et al., 2017). CALMODULIN BINDING PROTEIN 60g (CBP60g), a plant-specific transcriptional factor, along with its closely related gene SAR DEFICIENT 1 (SARD1) directly bind to the promoter of *ICS1* and activate *ICS1* expression. Both *cbp60g* and *sard1* mutants exhibit enhanced susceptibility to *Pma* ES4326 and *P. syringae* pv. *tomato* strain DC3000 (*Pst* DC3000) (Wang et al., 2011; Sun et al., 2015).

Without pathogens, it is important for plants to suppress pathogen responses so as to keep normal growth, and the SA concentration is maintained at basal level. Over accumulation of SA in plants causes constant activation of downstream immune response genes, which increases resistance against pathogens. However, the increased resistance trades off with plant growth (van Butselaar and Van den Ackerveken, 2020). For instance, constitutive expression of EDS1/PAD4 results in the accumulation of SA and immune response which increases the resistance to *Pst* DC3000 but also induced autoimmunity (Cui et al., 2017). CALMODULIN-BINDING TRANSCRIPTION FACTOR 3 (CMTA3) suppresses the expression of *CBP60g* and *SARD1*. In the triple mutants of *cmta1/2/3*, *PR1* and *PR2* are conspicuously activated, and the mutant plants size are extremely small comparing to the WT ( Sun et al., 2020).

As a transcription active marker, histone acetylation is also crucial for the SA signal pathway. The CBP/p300-family histone acetyltransferases (HATs), HAC1 and HAC5 (HAC1/5), form a complex with NPR1 and TGAs to activate *PRs* gene transcription by reprogramming the histone acetylation (Jin et al., 2018). HISTONE DEACETYLASE 19 (HDA19), an RPD3/HDA1-type deacetylase in Arabidopsis, directly binds to the promoter region of *PR1* and *PR2* to repress their expression (Choi et al., 2012). Previously, we found a strong allele mutation of another RPD3/HDA1-type deacetylase *HDA6*, named *shining 5* (*shi5*), exhibited autoimmune phenotypes such as cell death in the leaves and significantly reduced plant size (Wang et al., 2017), indicating that *HDA6* plays a vital role in repressing plant autoimmunity. However, the exact mechanism is not clear yet. Here, we reported that HDA6 could directly repress the expression of *SARD1* and *CBP60g* leading to the repression of SA biosynthesis, the upstream of the SA signal pathway, to maintain low SA levels for plant growth under normal conditions or to avoid excess immunity reactions when challenged by pathogens.

## Results

### The autoimmune phenotypes of *shi5* mutants depend on the SA pathway

The *shi5* mutants harbor a point mutation of *HDA6* with a C to T transition which changes the 277th serine to phenylalanine (S277F) located in the HDA domain (Wang et al., 2017). Under normal growth conditions, the *shi5* mutant plants showed the autoimmune phenotypes as hypersensitive cell death in leaves: tissue lesions from leaf margin to the center main veins, small plant size, and low fertility (Figure 1D; Wang et al., 2017). SA is a well-known defense-related hormone, the phenotypes of *shi5* might result from the disorder of the SA pathway in *shi5* mutants. To elucidate this possibility, we disrupted the SA pathway in *shi5* mutants by creating the double mutants of *ics1 shi5* to eliminate SA biosynthesis or *npr1 shi5* to rupture the conduction of SA signals. Not surprisingly, the double mutants of both *ics1 shi5* and *npr1 shi5* lost the leaf tissue
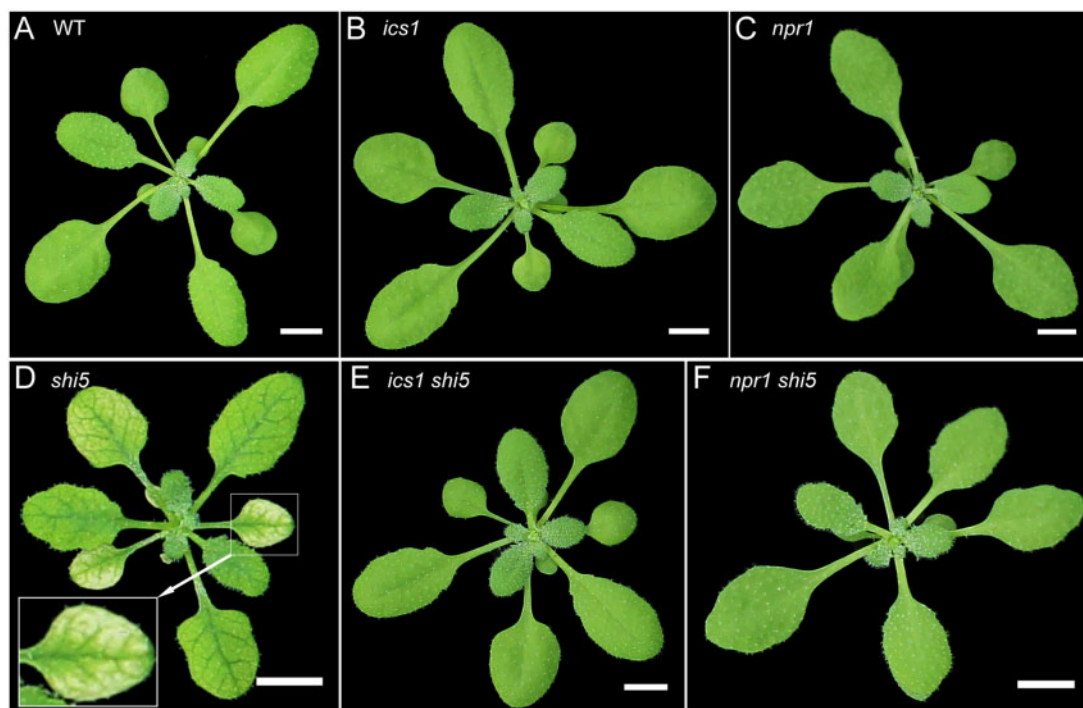
**Figure 1** The autoimmune phenotypes of *shi5* mutants rely on the SA-signal pathway. Pictures of ∼4-week-old WT (A), *ics1* (B), *npr1* (C), *shi5* (D), *ics1 shi5* (E), and *npr1 shi5* (F) mutants. White boxes in (D) show amplification of the small leaf with obvious HR cell death phenotype. Bar = 0.5 cm.

lesion phenotypes compared to *shi5* single mutants (Figure 1, D–F), and no yellowish in their leaves, almost indistinguishable from *ics1* or *npr1* single mutants respectively. Besides, the plant size of *ics1 shi5* resembled *ics1* single mutants (Figure 1, A, B, and E). The size of *npr1 shi5* double mutants was still a little smaller than *npr1*, but much bigger than *shi5* single mutants. The leaf shape of *npr1 shi5* behaved similarly to *npr1* single mutants (Figure 1, C and F). The similar phenotypes between *ics1 shi5*, *npr1 shi5* double mutants and *ics1*, *npr1* single mutants, respectively, indicate that the spontaneous HR in *shi5* caused by *HDA6* mutation highly depends on the SA signal pathway.

Furthermore, *shi5* mutants also displayed significantly more resistance to *Pst* DC3000 comparing to WT plants (Figure 2, A and B), and enormous de-repression of pathogen-response genes such as *PR1*, *PR2*, and so on (Wang et al., 2017). *PR1* and *PR2* are two downstream targets of the SA pathway, and their expression is highly activated by SA when plants are infected by pathogens (Nawrath and Metraux, 1999; Zhang et al., 1999). To determine whether the high resistance to *Pst* DC3000 of *shi5* mutants also relates to SA, we performed the *Pst* DC3000 inoculation test with single and double mutants of *ics1 shi5* and *npr1 shi5*. As expected, *shi5* single mutants were more resistant to *Pst* DC3000, while both *ics1* and *npr1* single mutants exhibited much higher susceptibility than the WT plants (Figure 2, A and B). Surprisingly, the double mutants of *ics1 shi5* and *npr1 shi5* behaved even more vulnerable to

*Pst* DC3000 than the *ics1* and *npr1* single mutants (Figure 2, A and B). We also examined the expression of *PR1* and *PR2* in these mutants. Before inoculation, *PR1* and *PR2* were highly de-repressed in *shi5* mutants compared to WT plants (Figure 2, C and D). However, their expression in the *ics1 shi5* and *npr1 shi5* double mutants resembled to that of *ics1* and *npr1* which was far lower than WT plants (Figure 2, C and D), suggesting the de-repression of *PR1* and *PR2* expression by *HDA6* mutation is depending on the SA pathway, as attenuation of the SA pathway aborts *PR1* and *PR2* de-repression in *shi5*. After *Pst* DC3000 inoculation, *PR1* and *PR2* in the *shi5* mutants were also greatly activated and higher than that in WT plants (Figure 2, C and D), meaning *HDA6* still represses *PR1* and *PR2* expression during infection. In the single mutants of *ics1* and *npr1*, *PR1* and *PR2* expression were drastically reduced compared to WT plants or *shi5* mutants, especially for *PR1* in the *ics1* mutants which fell to almost as low as the mock control (Figure 2, C and D), consistent with the role of SA for activating *PR1* and *PR2* during pathogen infection. Intriguingly, when checking closely, the expression of *PR1* and *PR2* in the double mutants of *npr1 shi5* and *ics1 shi5* was less than in the *npr1* and *ics1* single mutants, respectively (Figure 2, C and D), which is consistent with the higher susceptibility to *Pst* DC3000 of *npr1 shi5* and *ics1 shi5* double mutants (Figure 2, A and B), suggesting that the de-repression of *PR1* and *PR2* during pathogen infection in *shi5* is also SA dependent.
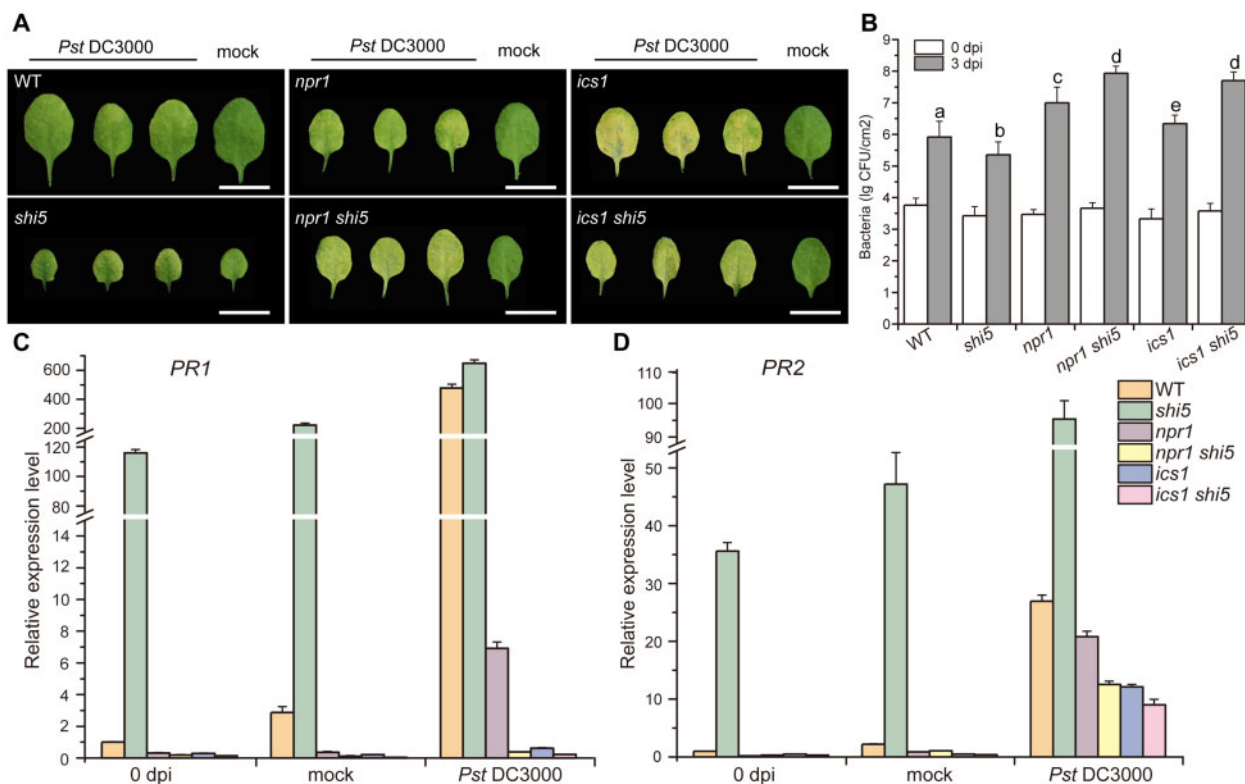
**Figure 2** The high resistance to *Pst* DC3000 of *shi5* mutants depends on the SA-signal pathway. A, Leaf phenotypes after *Pst* DC3000 infection. Leaves were collected 3-d post inoculation (dpi). Mock: MgSO4 medium infiltrated. Bar = 1 cm. B, Quantification of bacteria from the inoculated leaves. Leaves were harvested 3 dpi. 0 dpi: Infiltrated leaves were immediately harvested after inoculation. The error bars show SD (*n* = 8). Letters on the columns indicate the statistically significant differences by the one-way ANOVA (analysis of variance) test (*P* < 0.05). C and D, Expression of *PR1* (C) and *PR2* (D) in the WT, *shi5*, *npr1*, *npr1 shi5*, *ics1*, and *ics1 shi5* before *Pst* DC3000 inoculation or at 24-h post-inoculation. The expression is relative to the WT plants at 0 dpi. Error bars indicate the SD of three biological replicates.

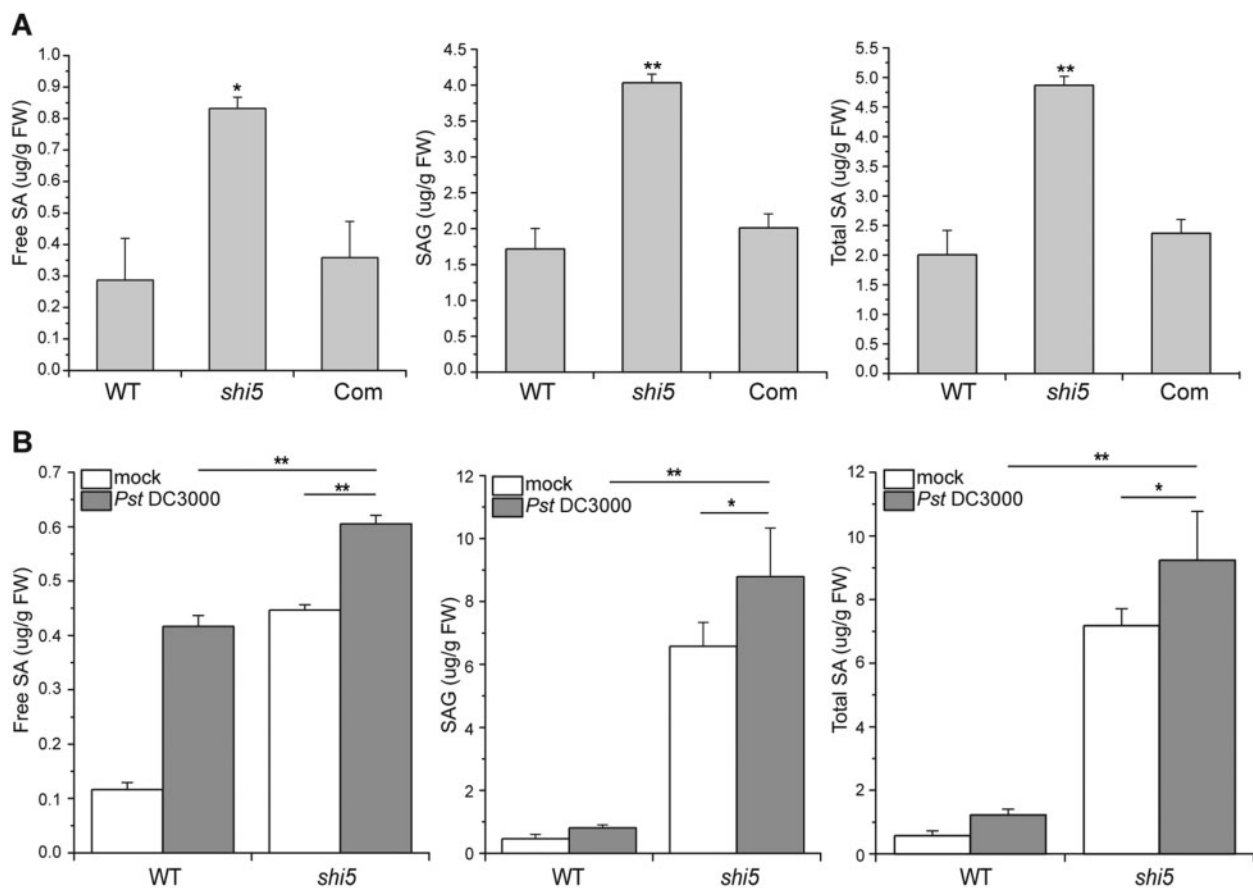## SA is accumulated in *shi5* mutants

To investigate how *HDA6* influences the SA pathway to repress the expression of downstream genes. We first quantified the SA concentration in WT, *shi5* mutants and a complemental line which contains a native *HDA6* promoter driving *HDA6:FLAG* fusion gene in *shi5* background. Both the free SA and the conjugated SA were highly accumulated, correspondingly with much higher total SA levels in *shi5* mutants, while in the complemental line, the elevated SA in *shi5* was restored to the similar levels as WT plants (Figure 3A), which indicates that SA accumulation is repressed by *HDA6* under normal growth conditions.

When invaded by pathogens, SA was quickly synthesized to induce downstream counter-pathogen reactions (Janda and Ruelland, 2015). It is interesting to know whether HDA6 also regulates SA accumulation during pathogen infection or not, so we examined the SA level in WT plants and *shi5* mutants infected by *Pst* DC3000. As expected, in WT plants, SA, especially the free SA concentration increased obviously after treated with *Pst* DC3000 (Figure 3B). In *shi5* mutants, although SA was already conspicuously accumulated compared to WT plants, the concentration of free SA and conjugated SA, as well as

total SA, raised significantly by *Pst* DC3000 infection like WT plants (Figure 3B), indicating that pathogen infection can still induce SA accumulation under *HDA6* attenuation. When comparing these two genotypes, the infected *shi5* mutants accumulated much more SA than infected WT plants (Figure 3B), consistent with its high resistance to *Pst* DC3000. These results also suggested that *HDA6* represses SA accumulation during pathogen infection to prevent excessive SA production to overreact against pathogen attacks.

## HDA6 represses the *ICS1* SA biosynthesis pathway

To determine whether the SA accumulation in *shi5* mutants is related to SA biosynthesis and which pathway is affected by *HDA6* mutation, we further checked the expression of *ICS1* and *PAL1*, the key enzymes of two SA biosynthesis pathways, in WT, *shi5*, and complemental line. It was found that *ICS1* but not *PAL1* was de-repressed in *shi5* mutants compared to the WT and complemental line (Figure 4A), indicating that only the *ICS1* pathway is regulated by *HDA6*. This is understandable as *shi5* mutants exhibit plant immunity-related phenotypes and the *ICS1* pathway is more relevant to plant immunity (Wildermuth

**Figure 3** SA is accumulated in *shi5* mutants under normal conditions or infected by *Pst* DC3000. A, SA quantification in WT, *shi5* mutants, and *HDA6* complemental line. Left: free SA, Middle: SAG, Right: total SA. FW, fresh weight. B, SA quantification in WT and *shi5* mutants at 24-h post *Pst* DC3000 inoculation. Error bars show SD of three biological replicates. Asterisks indicate statistically significant differences (*$P < 0.05$, **$P < 0.01$ in the Student's *t* test).

et al., 2001; Dempsey et al., 2011), and the functional disruption of *ICS1* in *shi5* mutants could reverse the immunity phenotypes of *shi5* (Figure 1). Consistent with the SA levels in plants, *ICS1* expression was induced by *Pst* DC3000 infection, and higher expression of *ICS1* was detected in *shi5* mutants under both infection and no-infection conditions (Figure 4F).

### HDA6 suppresses the expression of *CBP60g* and *SARD1*

To investigate how HDA6 represses *ICS1* expression, we examined the expression of SA regulators upstream of *ICS1* (Dempsey et al., 2011). The transcription of *CBP60g* and *SARD1* got the highest scale of de-repression in *shi5* mutants (Figure 4B), while other regulators such as *NDR1*, *EDS1*, *PAD4*, *SAG101*, and *EDS5* showed about the same scale of expression as *ICS1* in *shi5* mutants (Supplemental Figure S1A). Some regulators such as *EIN3* and *EIL1*, also involved in the ethylene pathway, were almost not influenced by HDA6 mutation (Supplemental Figure S1A), indicating HDA6 may not regulate the ethylene pathway.

As the released *ICS1* expression in *shi5* mutants was still induced by *Pst* DC3000 infection, we examined the expression of *CBP60g* and *SARD1* in the WT plants and *shi5* mutants with *Pst* DC3000 inoculation. Like the expression of *ICS1* (Figure 4F) as well as SA level (Figure 3B) changes, the expression of *CBP60g* and *SARD1* were induced by pathogen treatments in both backgrounds, but much higher in *shi5* mutants (Figure 4, C and D), suggesting HDA6 represses *CBP60g* and *SARD1* expression under both normal and pathogen attack conditions. It is intriguing that *PBS3*, another key enzyme just downstream of *ICS1* in the *ICS1* SA synthesis pathway, also was obviously de-repressed in *shi5* mutants and induced by *Pst* DC3000 infection (Figure 4B). While, unlike *CBP60g* and *SARD1*, upon pathogen infection, *PBS3* expression in *shi5* is less than that in WT plants (Figure 4E), indicating *PBS3* is differently regulated from *CBP60g* and *SARD1* when challenged by pathogens.

As mutation of HDA6 causes de-repression of *CBP60g* *SARD1* and *ICS1*, it is intriguing to know how overexpression of *HDA6* affects the transcription of these genes. We
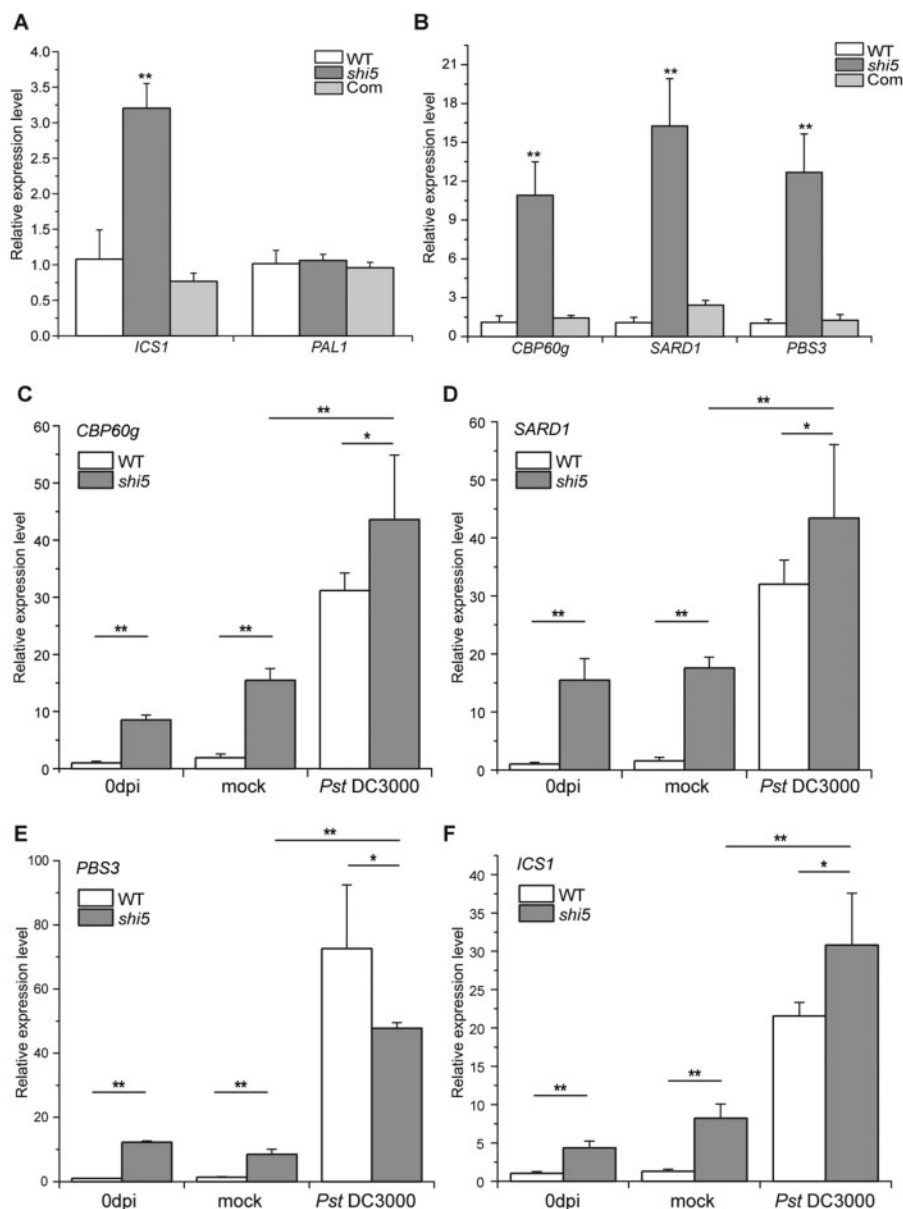
**Figure 4** HDA6 represses the expression of ICS1 and its activator CBP60g SARD1. A, Expression of ICS1 and PAL1, two key enzymes in the plant SA biosynthesis pathway, in WT, shi5 mutants and HDA6 complemental line under normal conditions. The expression is relative to the WT plants. B, Expression of CBP60g, SARD1, and PBS3 in WT, shi5 mutants, and complemental line under normal condition. The expression in WT plants was set 1.0. C–F, Expression of CBP60g (C), SARD1 (D), PBS3 (E), and ICS1 (F) before Pst DC3000 inoculation or at 24-h post-inoculation. The expression is relative to the WT plants at 0 dpi. Error bars indicate the SD of three biological replicates. Asterisks indicate statistically significant differences (*P < 0.05, **P < 0.01 in the Student's t test).

checked their expression in an HDA6 overexpression transgenic line. Compared to WT plants, CBP60g was significantly suppressed in HDA6-OE line, although statistically no significant changes were observed for SARD1 and ICS1, their transcription was slightly lower than the WT (Supplemental Figure S1B).

## CBP60g and SARD1 are direct targets of HDA6
Whether the released expression of ICS1 in shi5 mutants is due to the direct de-repression by HDA6 mutation or indirectly results from the de-repression of ICS1 activators such

as CBP60g and SARD1 is not clear. To address this question, we first quantified the histone acetylation levels at the promoter regions of ICS1, CBP60g, and SARD1 by chromatin immunoprecipitation (ChIP) against histone H3 acetylation (H3Ac) following quantitative polymerase chain reaction (PCR) checking. Consistent with much higher expression of CBP60g and SARD1 in shi5 mutants, significantly higher histone H3Ac enrichment was observed in the distal promoter region of both CBP60g and SARD1 in shi5 mutants compared to control plants, while the proximal promoter region and intron region of CBP60g and SARD1 showed no obvious
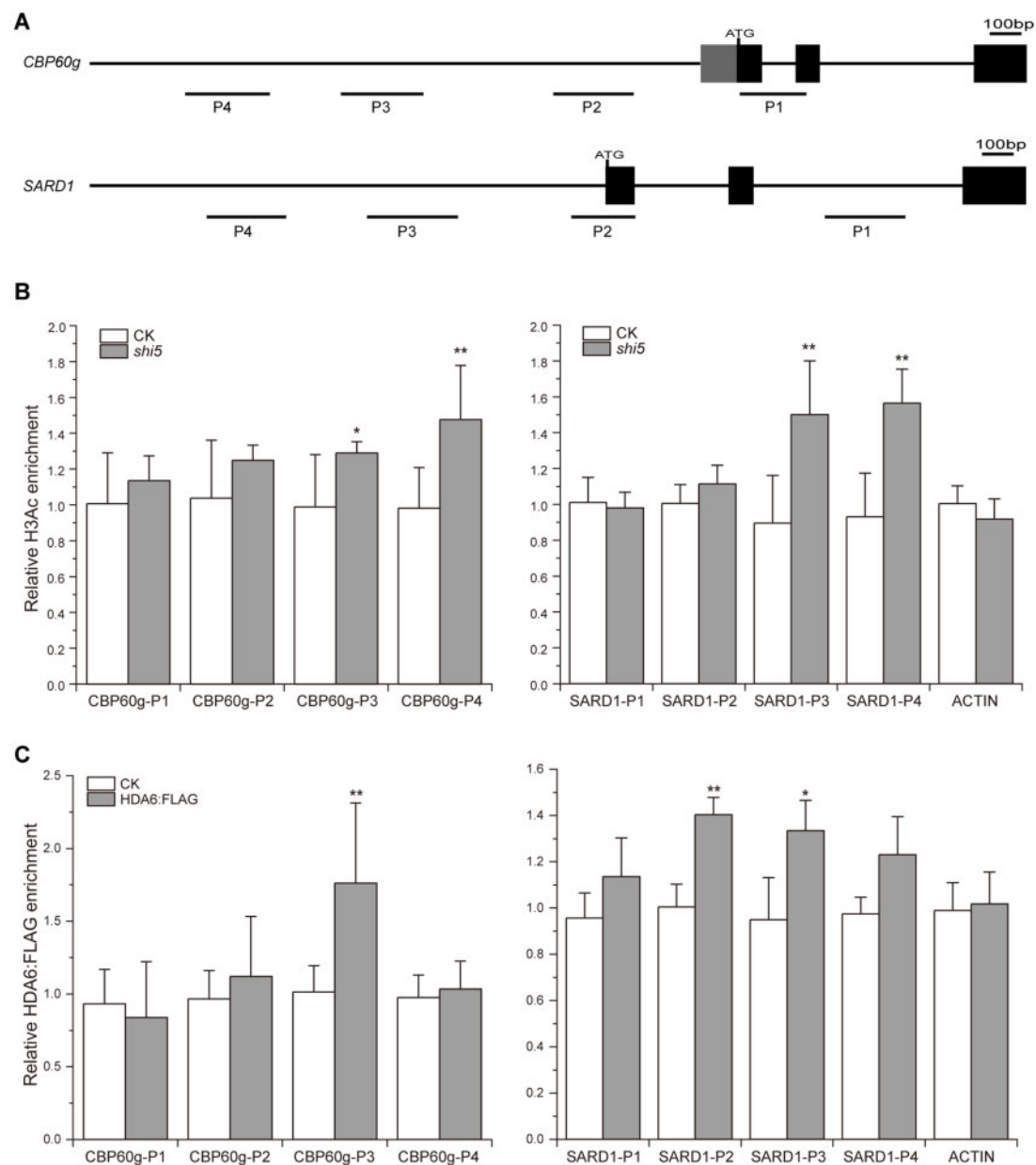
**Figure 5** *CBP60g* and *SARD1* are the direct targets of *HDA6*. A, Schematics of the promoter and partial genomic region for *CBP60g* and *SARD1* for ChIP assays. Black and gray boxes represent exons and 5′-untranslated regions, respectively. Solid lines indicate 5′-upstream promoters or introns. Dark lines below show fragments for quantitative PCR examination. ATG above the boxes shows the translation start site. B, Relative histone H3Ac enrichments within *CBP60g* and *SARD1* chromatin in CK and *shi5* mutants determined by ChIP-qPCR. The enrichment for each fragment is relative to the respective CK level. The error bars show the SD of three biological replicates. *ACTIN* was used as a negative control. CK, control of WT. C, Relative HDA6:FLAG binding to *CBP60g* and *SARD1* chromatin. The enrichment for each fragment is relative to the respective CK level. The error bars show the SD of three biological replicates. *ACTIN* was used as a negative control. CK, WT without HDA6:FLAG. Asterisks indicate statistically significant differences (*$P < 0.05$, **$P < 0.01$ in the Student's $t$ test).

enrichment (Figure 5, A and B). Different from *CBP60g* and *SARD1*, low enrichment of H3Ac was detected in the promoter of *ICS1*, with no significant difference between *shi5* mutants and control plants (Supplemental Figure S2, A and B), suggesting that the release of *ICS1* in *shi5* is not directly related to the histone acetylation status of *ICS1* promoter.

Then, to check whether HDA6 could directly bind to these genes, we performed another ChIP using antibody against the HDA6:FLAG fusion protein. Both *CBP60g* and *SARD1* promoter regions showed significant HDA6 binding (Figure 5C). No obvious HDA6 binding was found in the promoter of *ICS1* (Supplemental Figure S2C). Considering much higher expression of *CBP60g* and *SARD1* than *ICS1* in *shi5*, the significant H3Ac enrichment in the promoter of *CBP60g* and *SARD1* but not *ICS1*, the direct binding of HDA6 to *CBP60g* and *SARD1* promoter, together with the

previous report that *CBP60g* and *SARD1* directly activate *ICS1* expression (Wang et al., 2011; Sun et al., 2015), it is very likely that *HDA6* represses the expression of *ICS1* to regulate SA biosynthesis mainly through the suppression of *CBP60g* and *SARD1*. Unlike *CBP60g* and *SARD1*, neither significant H3Ac enrichment nor significant HDA6 binding on the *PBS3* promoter region was detected (Supplemental Figure S2, B and C), further implying *PBS3* might be regulated in a different way to *CBP60g* and *SARD1*.

### CBP60g and SARD1 mutation alleviate the immunity phenotypes of shi5 mutants

*CBP60g* and *SARD1* function redundantly for the activation of *ICS1* expression to induce SA biosynthesis (Sun et al., 2015). At the molecular level, HDA6 directly represses *CBP60g* and *SARD1* expression. To analyze the genetic interactions among *CBP60g*, *SARD1*, and *HDA6*, the double mutants of *cbp60g shi5*, *sard1 shi5* and triple mutants of *cbp60g sard1 shi5* were created, and their phenotypes were scored. Comparing to *shi5* single mutants, the double mutants *cbp60g shi5* and *sard1 shi5* both exhibited leaf yellowish phenotype, while leaves of the *cbp60g sard1 shi5* triple mutants were almost restored to WT plants although the plant size was still smaller than WT plants (Figure 6A). Consistent with the leaf phenotypes, the expression of *ICS1* in double mutants was obviously less than in *shi5* single mutants, and that in *cbp60g sard1 shi5* triple mutants was significantly lower than in *cbp60g shi5* or *sard1 shi5* double mutants (Figure 6B). This was consistent with the redundancy role of *CBP60g* and *SARD1* in *ICS1* activation.

When looking at phenotypes of response to pathogen, corresponding to the SA levels in plants, the *shi5* single mutants displayed resistance to *Pst* DC3000, while distinct higher susceptibility was observed in *cbp60g sard1* double mutants compared to WT plants as expected (Figure 7, A and B). The *cbp60g sard1 shi5* triple mutants behaved like *cbp60g sard1* double mutants with high susceptibility to *Pst* DC3000 (Figure 7, A and B). The *ICS1* expression in these samples was examined. Both before and after *Pst* DC3000 treated, *ICS1* expression was clearly de-repressed in *shi5* single mutants compared to WT plants; however, this de-repression was almost inhibited in the *cbp60g sard1 shi5* triple mutants (Figure 7C) indicating the repression of *ICS1* by *HDA6* mainly depends on *CBP60g* and *SARD1*. All these evidence suggested that *CBP60g* and *SARD1* are just genetically downstream of *HDA6*, and their expression is directly repressed by *HDA6*.

### The transcriptome of shi5 mutants mimics that of exogenous SA treated or Pma ES4326-infected plants

To better understanding the function of *HDA6* for plant immunity regulation, we checked the transcriptome variations between the *shi5* mutants and WT plants (as control) by transcriptome sequencing (RNA-sequencing [RNA-seq]). Three biological repeats seedlings were used as materials

(see "Materials and methods"). The samples of control and *shi5* mutant plants were clearly separated into two distinct groups at the PC1 dimension by principle component analysis (Supplemental Figure S3B). Consistent with the role of *HDA6* in repressing gene expression, the gene expression profiles in *shi5* mutants were broader than that in the control plants (Supplemental Figure S3A), and much more genes show elevated expression than genes with decreased expression in *shi5* mutants (Figure 8B; Supplemental Figure S3C). Gene's expression difference ⩾2-fold or ⩽0.5-fold with false discovery rate (FDR) < 0.05 were set as upregulated or downregulated differentially expressed genes (DEGs). Compared to the control plants, 2,529 upregulated, 660 downregulated, and a total of 3,189 DEGs were identified (Figure 8A; Supplemental Table S1). As *HDA6* is well known for its function for gene repression, we focused on the upregulated DEGs in *shi5* mutants. We performed the gene ontology (GO) and KEGG (Kyoto Encyclopedia of Genes and Genomes) pathway enrichment analysis with these upregulated DEGs. The KEGG analysis result showed that the plant–pathogen interaction pathway got the most significant enrichment (with the smallest q-value), and the plant hormone signal transduction pathway was also significantly enriched (Figure 8C; Supplemental Table S2). For GO analysis, the top 10 significant enriched GO terms of biological process were all about responding to stress or stimulus, and GO terms related to plant–pathogen response such as innate immune response, response to SA, SAR, and plant-type HR were among the top 50 significantly enriched terms (Supplemental Figure S4; Supplemental Table S3), which supported the role of *HDA6* in regulating plant response to environmental stresses especially to pathogen challenge, and also might explain why *HDA6* mutation in *shi5* results in such severe plant immunity phenotypes.

To further illustrate the relationship between SA accumulation and the transcriptome in *shi5* mutants, we compared the DEGs in *shi5* with that in plants applied with exogenous SA (Ding et al., 2018). A significant overlap was observed (Figure 9A). More than a half of SA-induced genes were presented in upregulated genes in *shi5*, and a great portion of common DEGs was also shared between SA-repressed genes and downregulated genes in *shi5* (Figure 9A). Very similar results were got when comparing DEGs in *shi5* with those in *Pma* ES4326-infected plants (Zhou et al., 2018; Figure 9B) as pathogens attack may trigger SA synthesis in plants. These results suggested that the transcriptome of *shi5* mutants mimics that of exogenous SA or *Pma*-treated plants, and the effect of gene expression by *HDA6* mutation largely results from SA accumulation in the *shi5* mutants. We also checked the overlapping between upregulated genes in *shi5* mutants with upregulated or downregulated genes in *Pma* treated *sid2* mutants (*ICS1* mutated) versus *Pma* treated WT plants. More than two-third (242 out of 357 genes) of downregulated genes in *sid2* were presented in the upregulated genes in *shi5*, indicating the significant overlap between these two categories, with $P < 2.155e{-}182$ by Fisher's
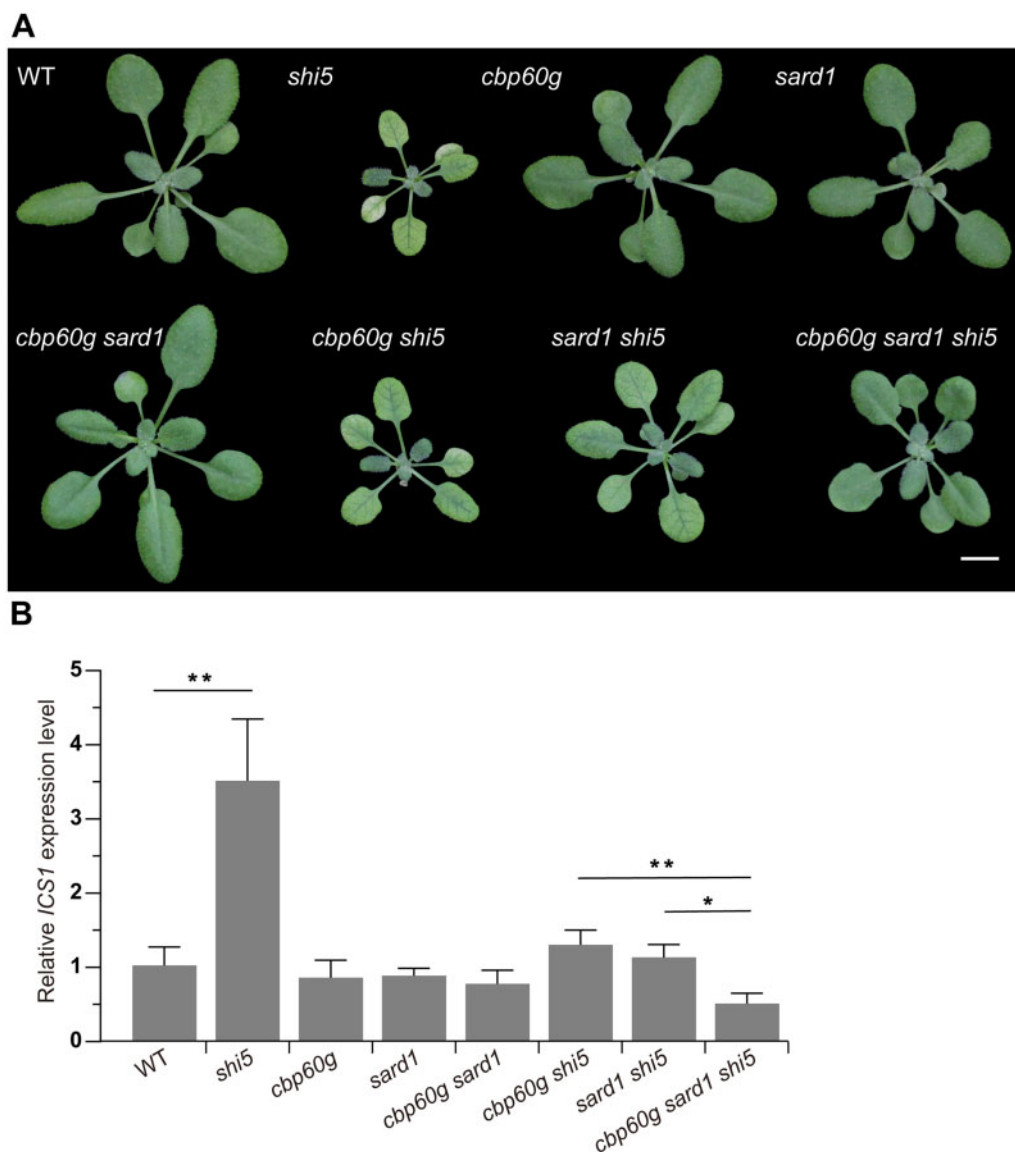
**Figure 6** *CBP60g* and *SARD1* mutation could alleviate the immunity phenotypes of *shi5* mutants. A, Pictures of WT, single mutants of *shi5*, *cbp60g*, *sard1*, double mutants of *cbp60g sard1*, *cbp60g shi5*, *sard1 shi5*, and triple mutants of *cbp60g sard1 shi5*. Bar = 1 cm. B, Relative expression of *ICS1* in WT, *shi5*, *cbp60g*, *sard1* single mutants, *cbp60g sard1*, *cbp60g shi5*, *sard1 shi5* double mutants, and *cbp60g sard1 shi5*. triple mutants. The expression is relative to the WT plants. The error bars show the SD of three biological replicates. Asterisks indicate statistically significant differences (*$P < 0.05$, **$P < 0.01$ in the Student's *t* test).

exact test (Figure 9C). Further analysis of these 242 genes showed that the top 10 enriched biological process were SA and pathogen response-related (Figure 9E; Supplemental Table S3), and among them, a big portion of genes related to response to SA showed obviously de-repression in *shi5* mutants (Figure 9D), suggesting that SA synthesized through the *ICS1* pathway for plant response to pathogens may account for gene de-repression in *shi5* mutants.

### HDA6 is induced by exogenous SA or *Pst* DC3000 infection

HDA6 suppresses SA biosynthesis under normal conditions or infected by pathogens. It is interesting to know whether *HDA6* itself is regulated by SA or pathogens. We examined the expression of *HDA6* in plants after exogenous SA treatment or inoculated with *Pst* DC3000. Intriguingly, both treatments could induce *HDA6* expression (Supplemental Figure S5, A and B). Since *Pst* DC3000 infection highly induces the expression of *CBP60g* and *SARD1*, consistent with the transcription, the enrichment of histone H3Ac on their promoter was increased for both control plants and *shi5* mutants (Supplemental Figure S5C). Then we wondered whether the inducing of *HDA6* by pathogens could alter its binding on the *CBP60g* and *SARD1* chromatin, and whether their increasing transcription past infection results from release the binding of HDA6 on their promoter. Not as expected, after *Pst* DC3000 infection, HDA6 was still enriched in the promoter of *CBP60g* and *SARD1* without
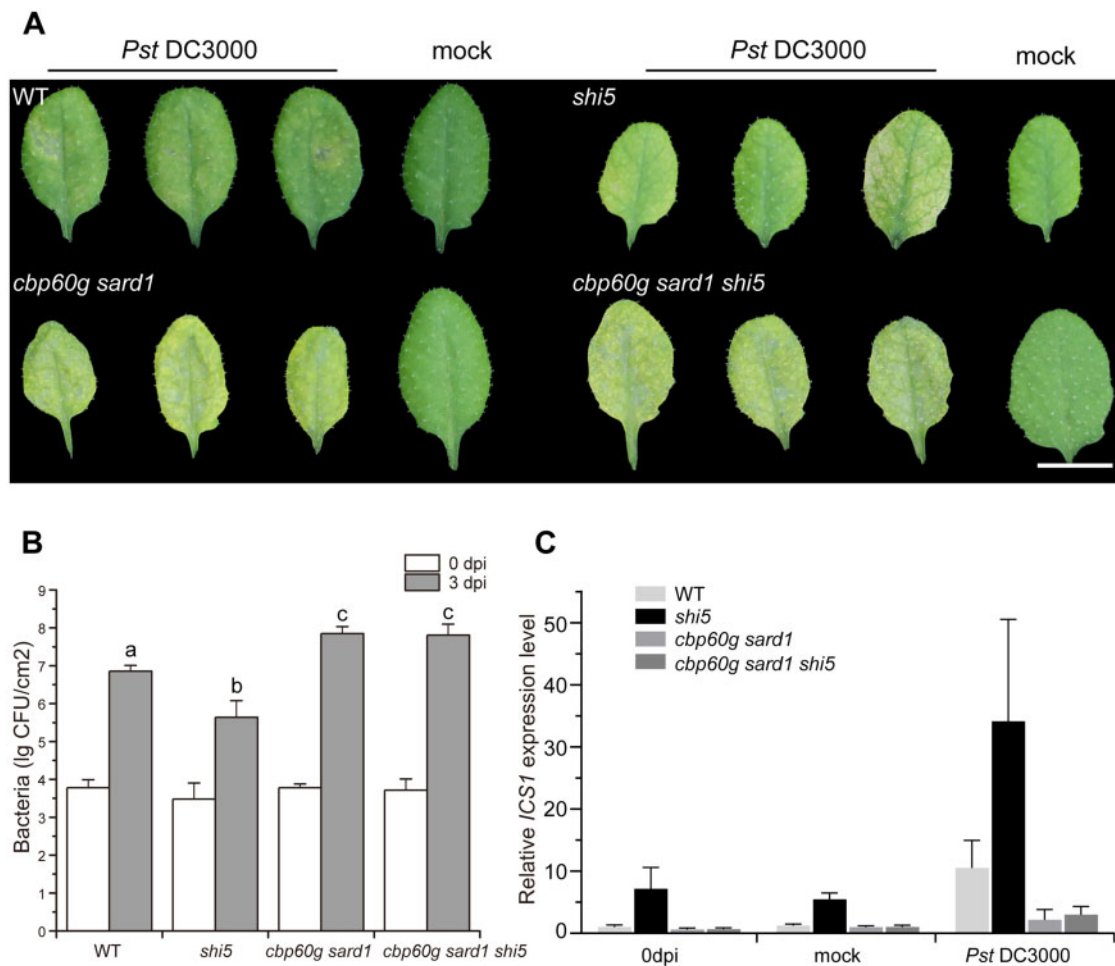
**Figure 7** *CBP60g* and *SARD1* contribute to the high resistance to *Pst* DC3000 of *shi5* mutants. A, Leaf phenotypes after *Pst* DC3000 infection. Leaves were collected 3 dpi. Mock: MgSO4 medium infiltrated. Bar = 1 cm. B, Quantification of bacteria from the inoculated leaves. Leaves were harvested 3 dpi. 0 dpi: Infiltrated leaves were immediately harvested after inoculation. The error bars show SD (*n* = 8). Letters on the columns indicate the statistically significant differences by the one-way ANOVA test (*P* < 0.05). C, Relative expression of *ICS1* in WT, *shi5*, *cbp60g sard1* double, and *cbp60g sard1 shi5* triple mutants before *Pst* DC3000 inoculation or at 24-h post-inoculation. The expression is relative to the WT plants at 0 dpi. Error bars indicate the SD of three biological replicates.

significant alteration (Supplemental Figure S5D), meaning that during pathogen challenging, HDA6 is also recruited although both genes are greatly induced. Considering much higher expression of *CBP60g* and *SARD1* (Figure 4) and more SA produced (Figure 3) in *shi5* mutants upon infection, HDA6 still performs its role for suppressing SA biosynthesis after pathogen infection. Thus, our data indicated that there may be a negative feedback loop formed as for SA pathway regulation by HDA6 to avoid excess responses when plants are attacked by pathogens.

## Discussion

As a major plant hormone, SA is critical for plants to fight against the pathogen infection (Kumar, 2014). The SA concentration in plants must be strictly controlled under normal conditions as well as when attacked by pathogens; however, the mechanisms are not well understood yet. Here we found that HDA6, a general gene repressor, plays a vital role in SA regulation. HDA6 suppresses SA biosynthesis under normal conditions or infected by pathogen, mainly through the direct repression of *ICS1* activator, *CBP60g* and *SARD1* for both conditions.

*CBP60g* and *SARD1* were highly de-repressed in *shi5* mutants, leading to significant accumulation of SA without pathogens. *Pst* DC3000 infiltration dramatically induced *CBP60g* and *SARD1* expression so caused fast SA accumulation both in the control and in *shi5* (Figures 3 and 4). But if consider fold-wise, the control plants and *shi5* mutants showed similar patterns of changes, which suggested the attenuation of HDA6 does not obviously alter plant ability to respond to pathogens. However, there were much higher expression of *CBP60g* and *SARD1* so more SA accumulated in *shi5* comparing to the control upon infection, and correspondingly more resistance to *Pst* DC3000 of *shi5* mutants, indicating *HDA6* mutation does increase the basal resistance against pathogens for plants, which is at the cost of plant growth as *shi5* has quite smaller plant size.
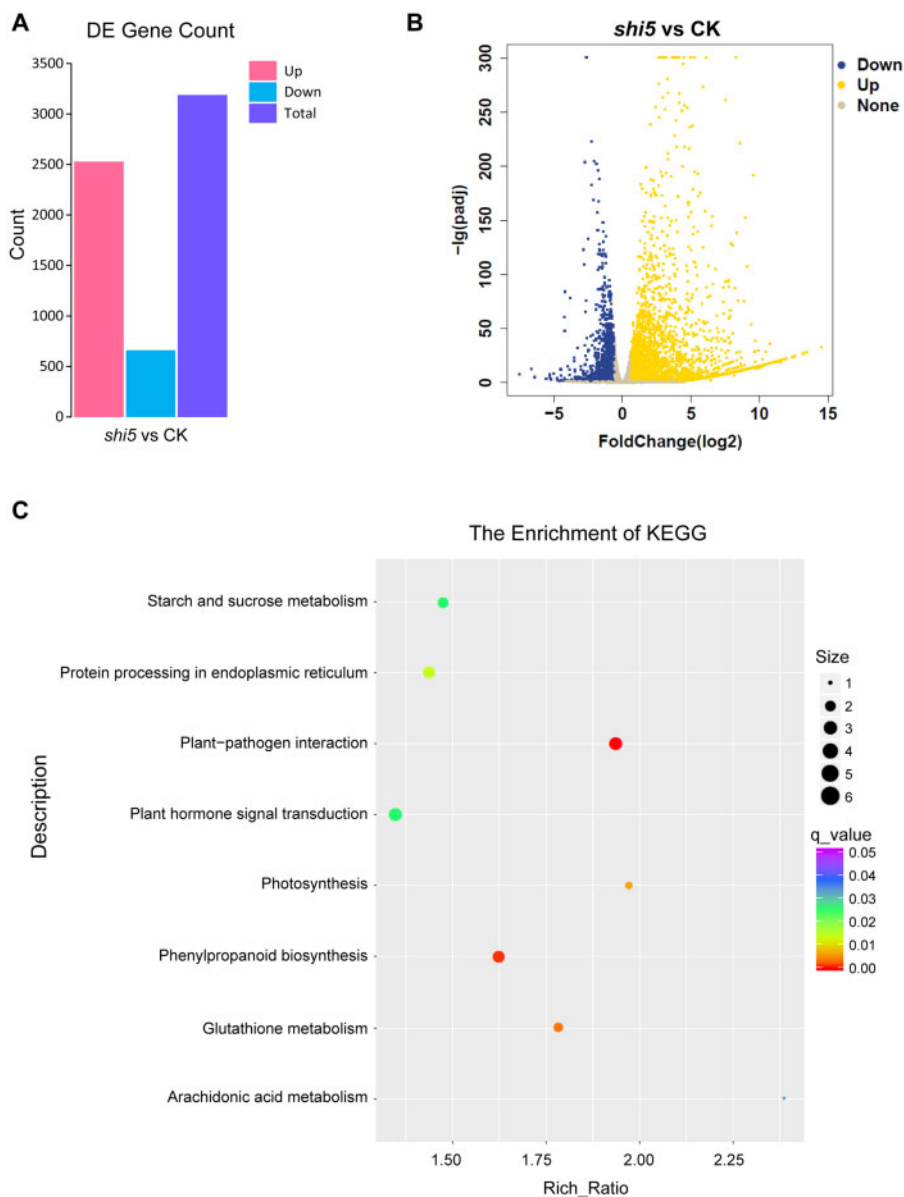
**Figure 8** The *shi5* mutants' transcriptome analysis. A, DEGs statistics of *shi5* compared to CK (WT plants). Gene's expression difference ⩾2-fold or ⩽0.5-fold with FDR < 0.05 were considered as up- or downregulated DEGs. Pink color, upregulated DEGs. Cyan color, downregulated DEGs. Blue color, total DEGs. B, Volcano map for the distribution of DEGs of *shi5* versus CK. Yellow represents significantly upregulated genes. Blue represents significantly downregulated genes. Gray represents no significantly changed genes. C, The KEGG pathway enrichment analysis of upregulated DEGs in *shi5* versus CK. Significantly enriched (with q < 0.05) pathways were presented. Color refers to the q-value, a lower q-value indicates more significance. Size refers to amount of genes enriched in the KEGG term.

Being the downstream of SA signal pathway, pathogen infection-induced *PR1* and *PR2* were greatly blocked when SA pathway was disrupted in the *npr1* or *ics1* mutants; correspondingly, the mutants were susceptible to pathogens. *PR1* and *PR2* were also increased in *shi5*. It is supposed that their expression in the double mutants of *npr1 shi5* and *ics1 shi5* will be higher than or similar to the *npr1* and *ics1* single mutants. While not as expected, in the double mutants *PR1* and *PR2* expression were much less than in the single mutants upon infection, and the double mutants were more susceptible to *Pst* DC3000 than the single respectively (Figure 2). As an active expression marker, histone acetylation status is balanced by the deacetylase and acetyl-transferases complex (HDAC and HAC). HDA6 dysfunction turns the balance to its antagonistic side which leads to the de-repression of its targets. Obviously, the antagonism effect on *PR1* and *PR2* in *shi5* was not working without SA, no matter this effect is direct or indirect. Indeed, in the previous report, SA was needed for inducing the HAC–NPR1–TGA HAT complex formation to activate *PR1* and *PR2* expression (Jin et al., 2018). Furthermore, the fold change of *PR1* and *PR2* induced by *Pst* DC3000 in the WT was bigger than in *shi5*, which may be due to the saturation of *PR1* and *PR2* in *shi5*.
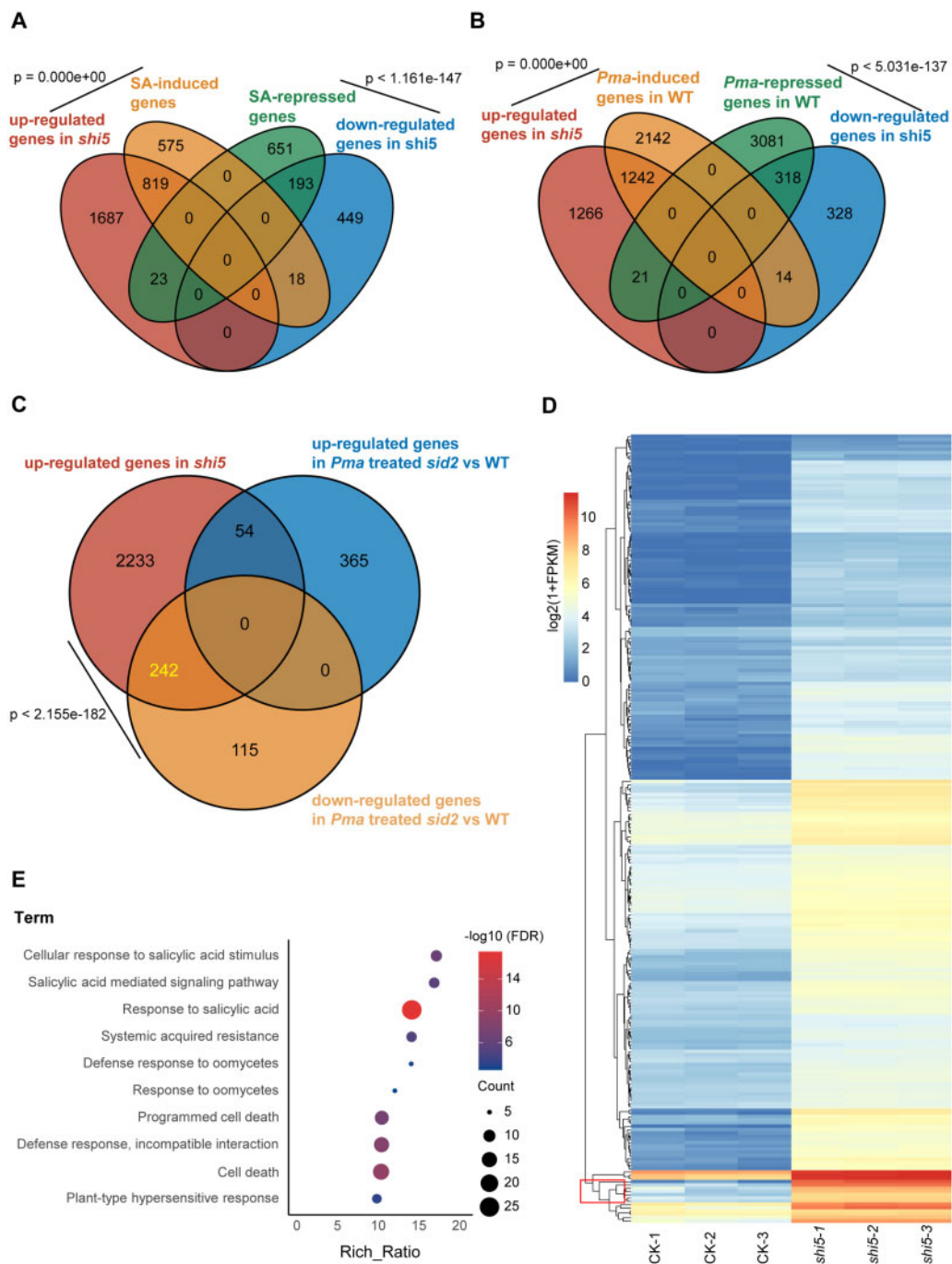
**Figure 9** The transcriptome of *shi5* mutants mimics that of exogenous SA treated or *Pma* ES4326 infected plants. A, Overlap of DEGs between *shi5* and exogenous SA treated plants. *P*-values show the statistical significance of the overlap between two groups of genes in Venn diagrams by Fisher's exact test. B, Venn diagram of the common DEGs between *shi5* and *Pma* ES4326 infected plants. *P*-values show the statistical significance of the overlap between two groups of genes by Fisher's exact test. C, Venn diagram of the common DEGs between upregulated genes in *shi5* and DEGs of *Pma* ES4326 treated *sid2* versus *Pma* ES4326-treated WT plants. *P*-value indicates the statistical significance of the overlap between two groups of genes by Fisher's exact test. D, Heatmap of the expression pattern of 242 common genes between upregulated DEGs in *shi5* and downregulated genes in *Pma* treated *sid2* versus WT. The heatmap shows value of log2-transformed [(average fragments per kilobase per million mapped fragments, FPKM) + 1] of each gene. Genes enclosed by red box belong to GO term of response to SA. E, Enrichment of biological process GO terms for the 242 common genes in (C) and (D). The top 10 significantly enriched terms with the highest rich ratio are presented.

Histone acetylation was enriched at the promoter region of *CBP60g* and *SARD1* in *shi5*, and HDA6 showed high binding on their promoters. While the peak seems to shift between histone acetylation enrichment and HDA6 binding

on the promoter regions of both genes. We speculated that this discrepancy may result from the steric effect. As a HDA, HDA6 lacks the ability to directly bind to DNA, it usually forms a multi-protein complex in which some components

perform the role for DNA binding (Ahringer, 2000; Grzenda et al., 2009). Then the chromatin binding sites might be a short distance away from the catalyzing site. However, does this deviation restrict to *CBP60g* and *SARD1* or is universal to other targets needs further illustration. Nevertheless, our data supported that HDA6 binds to *CBP60g* and *SARD1* promoter and directly suppresses their transcription.

Therefore, based on the data, we got here and previous reports, we proposed the role of *HDA6* in regulating plant immunity. In the absence of pathogen attack, the whole SA signal pathway has to be kept at the silence stage which enables normal growth for plants. To achieve the repression, HDA6 binds to the promoter of *SARD1* and *CBP60g* and deacetylates the histones to prevent their transcription which results in the repression of *ICS1* and impeding SA biosynthesis, thus silencing downstream genes such as *PR1* and *PR2*. When challenged by pathogens, induced *CBP60g* and *SARD1* promote *ICS1* expression which elevates SA levels to activate downstream *PRs* transcription. SA accumulation also raises *HDA6* expression, which may form a negative feedback loop, and HDA6 still functions for its suppression to avoid overreactions (Figure 10). But how pathogen infection or accumulated SA promotes *HDA6* expression is unclear and needs further investigation. Besides, although the tissue lesion phenotype is almost relieved in the *ics1 shi5* and *npr1 shi5* double mutants, the plant size of the double mutants is still slightly smaller than the single mutants, respectively, indicating HDA6 may be also involved in a SA independent pathway for plant immunity regulation, which requires further attention.

## Materials and methods

### Plant materials and growth conditions

Arabidopsis plants were grown in a soil mixture of vermiculite and peat soil (1:1 by volume) in the greenhouse under LD photoperiod with16-h light and 8-h dark, humidity ~60% at 22°C to 25°C. Plant seeds were first sterilized and sowed to half Murashige & Skoog (MS) solid medium to germinate and then transferred to soil. Mutants of *ics1* (also termed *sid2-2*, CS16438 of ABRC stock), *npr1* (*npr1-1*, CS3726 of ABRC stock), *cbp60g* (*cbp60g-1*, SALK_023199 of ABRC stock), and *sard1* (*sard1-2*, SALK_052422 of ABRC stock) were described previously (Cao et al., 1994; Wildermuth et al., 2001; Wang et al., 2011). The *HDA6* mutant *shi5*, the complemental transgenic line, and the overexpression line were the same as in our previous report (Wang et al., 2017). The double mutants of *ics1 shi5* and *npr1 shi5* were segregated from the F2 population of cross of *ics1* or *npr1* with *shi5*. The double and triple mutants of *cbp60g shi5*, *sard1 shi5*, and *cbp60g sard1 shi5* were segregated from the F2 population of cross of *cbp60g sard1* with *shi5*.

### SA quantification

The free SA and SA glucosidase (SAG) were extracted as previously described (Malamy et al., 1992; Choi et al., 2012) with minor revisions. In short, 0.5 g ~8 leaf-stage plants were harvested and ground to powder with liquid nitrogen, extracted with 90%, 100% methanol sequentially. The supernatant was combined, mixed well, and vacuum dried. The
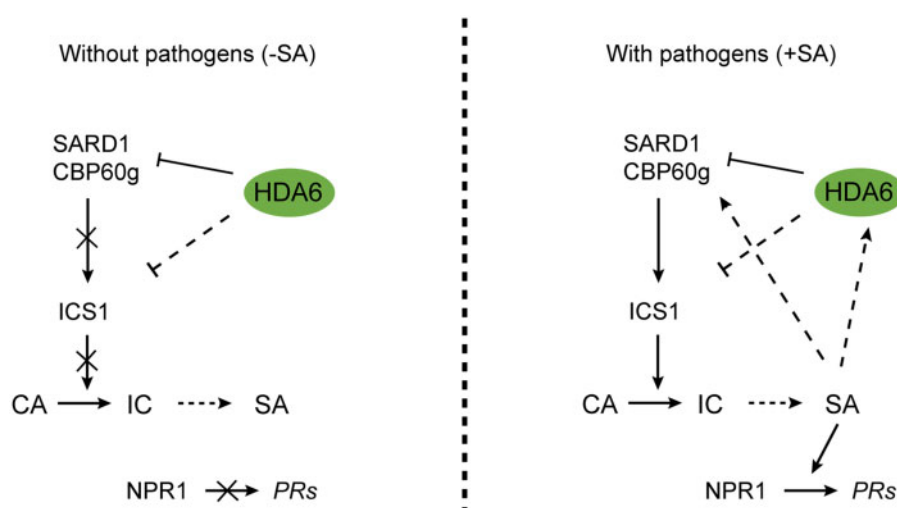


**Figure 10** Model for the role of *HDA6* in plant immunity. Without pathogen attack, HDA6 binds to the promoters of *CBP60g* and *SARD1* and deacetylates the histones to repress *CBP60g* and *SARD1* transcription, leading to the suppression of *ICS1* so as to inhibit SA biosynthesis. While infected by pathogens, the induced expression of *CBP60g* and *SARD1* activates the transcription of *ICS1* leading to the synthesis of SA. The newly synthesized SA may also activate the expression of *CBP60g* and *SARD1*. This positive feedback leads to the fast accumulation of SA which interacts with *NPR1* to promote PRs gene expression. However, during this process, *HDA6* expression is also induced and HDA6 still functions to prevent excessive production of SA and overreaction to the pathogens (right).

residues were re-suspended with 5% (w/v) trichloroacetic acid and partitioned using ethyl acetate:cyclopentane:isopropanol (50:50:1, v/v/v). The organic phase with free SA was vacuum dried and resolved in 50% methanol. The water phase was mixed with 5 mM sodium acetate buffer (pH 5.5) containing 40 U of β-glucosidase (Sigma, St Louis, MO, USA), 37°C 2 h, then acidized with 8 M HCl at 100°C 30 min and partitioned using ethyl acetate:cyclopentane:isopropanol (50:50:1, v/v/v). The organic phase was collected, vacuum dried, and resolved in 50% methanol for SAG analysis. The SA was separated by HPLC on a C18 column (250 × 4.6 mm, 5 μm, Agilent, St Clara, CA, USA) using a linear aqueous MeOH gradient from 10% to 82% (v/v), at a flow rate of 1 mL/min and quantified with fluorimetric detection (excitation at 305 nm; emission at 407 nm). The HPLC (high performance liquid chromatography) column was maintained at 40°C. All data were adjusted based on the recovery rate of spiked samples.

## RNA extraction and Real-time quantitative PCR (RT-qPCR)

RNA was extracted from leaves of ~8 leaf-stage soil growing plants. Trizol reagent (Invitrogen, Waltham, MA, USA) is used for RNA extract according to the manufacturer's instructions. For RT-qPCR, cDNAs were synthesized using Prime Script RT reagent Kit with gDNA Eraser (Takara, Shiga, Japan). RT-qPCR was performed on an ABI Prism 7900HT sequence detection system using AceQqPCR SYBR Green Master Mix (High ROX Premixed) Q141 (Nanjing, China), and TUB2 (AT5G62690) is used as the internal control. The primers used in this article are listed in Supplemental Table S4.

## Whole-genome RNA-seq and analysis

For the RNA-seq experiment, the soil-grown WT (as CK) and shi5 mutant plants at ~ 8 leaf stage were used as materials. Three biological replicates were used for analysis. Total RNA was extracted using the RNeasy Plus Mini Kit (Qiagen, Hilden, Germany) following the manufacturer's instructions. The RNAs were sequenced by Illumina HiSeq 2500 platform at the company Annoroad (Beijing, China). RNA-seq reads were aligned to the Arabidopsis reference genome (TAIR10) using HISAT2 (Kim et al., 2019) and gene-level raw count data files were generated using HTSeq (Anders et al., 2015). The DEGs were identified with Bioconductor package DESeq2 (Love et al., 2014) in R language with a fold change $\geqslant 2$ or $\leqslant 0.5$ with an FDR $\leqslant 0.05$. GO enrichment analysis was determined using agriGO (Tian et al., 2017). The RNA-seq data for exogenous SA treated plants was derived from BioProject PRJNA434313 in NCBI (Ding et al., 2018) and data for Pma ES4326-treated WT and sid2 mutants were from BioProject PRJNA390966 (Zhou et al., 2018).

## ChIP

ChIP experiments were carried out as described previously (Kaufmann et al., 2010). For ChIP against HDA6:FLAG, the WT plants and complemented shi5 mutants with HDA6:FLAG chimeric gene driven by the native HDA6 promoter were used as materials. In brief, total chromatin was extracted from 8 leaf-stage soil-growing plants, immunoprecipitated with rabbit polyclonal anti-FLAG antibody (catalog no. F7425, Sigma). By qPCR conduction, relative HDA6:FLAG enrichments were calculated after normalization to TUB8 (AT5G23860). For ChIP against histone acetylation, the WT and shi5 mutants were used. Total chromatin extracted from the same age plants as FLAG ChIP and immunoprecipitated with anti-acetylated histone H3 (catalog no. 06-599, Millipore) or histone H3 (ab1791, Abcam, Cambridge, UK). Relative enrichments of H3Ac were calculated after normalization to the H3 first. Each of the immunoprecipitations has three biological repeats, and each sample was quantified in triplicate.

## Pst DC3000 infection, bacteria count, and exogenous SA treatment

Pst DC3000 preparation and inoculation were performed as described previously (Wang et al., 2017). Pst DC3000 was grown at 28°C for 2 d on King's B agar plates supplemented with 50 mg/mL rifampicin. The single colonies were then inoculated into 5 mL of liquid King's B media and cultured to optical density $OD_{600} \geqslant 1$. The bacteria were collected by centrifugation, re-suspended in 10 mM $MgSO_4$ containing 0.01% Silwet L-77, and adjusted to $OD_{600} = 0.003$. The 8 leaf-stage soil-growing plants were inoculated through vacuum infiltration. About 3 d after, the fifth or sixth leaf was harvested to prepare leaf discs (3 mm in diameter) using a hole puncher. The leaf disc was ground in 10 mM $MgSO_4$. The homogenate was serial-diluted (1:10) and plated onto King's B medium containing 50 mg/mL rifampicin. The plate was incubated at 28°C for 2 d, then the colonies were counted for titrating calculation.

Exogenous SA treatment was performed as described with modifications (Ding et al., 2018). In short, 2-week-old seedlings were sprayed with 50 mM SA plus 0.05%(v/v) of Tween-20, and samples were collected for RNA extraction before (0 h) or 2 h after treatment with SA.

## Accession numbers

The raw RNA-seq data generated during this study were deposited in the National Center for Biotechnology Information (NCBI) database under the accession code PRJNA719986. Genes involved in this article are listed under the following accession numbers in the TAIR data libraries HDA6 (AT5G63110), CBP60g (AT5G26920), SARD1 (AT1G73805), ICS1 (AT1G74710), PBS3 (AT5G13320), PR1(AT2G14610), and PR2 (AT3G57260).

## Supplemental data

The following materials are available in the online version of this article.

**Supplemental Figure S1.** Quantification of SA accumulation-related gene expression in shi5 mutants and HDA6-OE line.

**Supplemental Figure S2.** The ChIP-PCR results for histone H3Ac enrichments and HDA6 binding on *ICS1* or *PBS3* chromatin.

**Supplemental Figure S3.** The transcriptome-sequencing results of *shi5* show the role of *HDA6* in gene repression.

**Supplemental Figure S4.** Enrichment of biological-process GO terms for the upregulated DEGs in *shi5* mutants.

**Supplemental Figure S5.** *HDA6* expression is induced by exogenous SA treatment or by *Pst* DC3000 infection.

**Supplemental Table S1.** DEGs in *shi5* mutants.

**Supplemental Table S2.** KEGG pathway enrichment report.

**Supplemental Table S3.** Results for the GO enrichment analysis.

**Supplemental Table S4.** Primers used in this article.

## References

**Ahringer J** (2000) NuRD and SIN3 histone deacetylase complexes in development. Trends Genet **16:** 351–356

**Anders S, Pyl PT, Huber W** (2015) HTSeq–a Python framework to work with high-throughput sequencing data. Bioinformatics **31:** 166–169

**Cao H, Bowling SA, Gordon AS, Dong X** (1994) Characterization of an Arabidopsis mutant that is nonresponsive to inducers of systemic acquired resistance. Plant Cell **6:** 1583–1592

**Choi SM, Song HR, Han SK, Han M, Kim CY, Park J, Lee YH, Jeon JS, Noh YS, Noh B** (2012) HDA19 is required for the repression of salicylic acid biosynthesis and salicylic acid-mediated defense responses in *Arabidopsis*. Plant J **71:** 135–146

**Cui H, Gobbato E, Kracher B, Qiu J, Bautor J, Parker JE** (2017) A core function of EDS1 with PAD4 is to protect the salicylic acid defense sector in *Arabidopsis* immunity. New Phytol **213:** 1802–1817

**Dempsey DA, Vlot AC, Wildermuth MC, Klessig DF** (2011) Salicylic Acid biosynthesis and metabolism. Arabidopsis Book **9:** e0156

**Ding P, Ding Y** (2020) Stories of salicylic acid: a plant defense hormone. Trends Plant Sci **25:** 549–565

**Ding Y, Sun T, Ao K, Peng Y, Zhang Y, Li X, Zhang Y** (2018) Opposite roles of salicylic acid receptors NPR1 and NPR3/NPR4 in transcriptional regulation of plant immunity. Cell **173:** 1454–1467 e1415

**Feys BJ, Moisan LJ, Newman MA, Parker JE** (2001) Direct interaction between the *Arabidopsis* disease resistance signaling proteins, EDS1 and PAD4. EMBO J **20:** 5400–5411

**Fu ZQ, Dong X** (2013) Systemic acquired resistance: turning local infection into global defense. Annu Rev Plant Biol **64:** 839–863

**Fu ZQ, Yan S, Saleh A, Wang W, Ruble J, Oka N, Mohan R, Spoel SH, Tada Y, Zheng N, Dong X** (2012) NPR3 and NPR4 are receptors for the immune signal salicylic acid in plants. Nature **486:** 228–232

**Grzenda A, Lomberk G, Zhang JS, Urrutia R** (2009) Sin3: master scaffold and transcriptional corepressor. Biochim Biophys Acta **1789:** 443–450

**Hofius D, Schultz-Larsen T, Joensen J, Tsitsigiannis DI, Petersen NH, Mattsson O, Jorgensen LB, Jones JD, Mundy J, Petersen M** (2009) Autophagic components contribute to hypersensitive cell death in *Arabidopsis*. Cell **137:** 773–783

**Huang W, Wang Y, Li X, Zhang Y** (2020) Biosynthesis and regulation of salicylic acid and N-hydroxypipecolic acid in plant immunity. Mol Plant **13:** 31–41

**Janda M, Ruelland E** (2015) Magical mystery tour: salicylic acid signalling. Environ Exp Bot **114:** 117–128

**Jin H, Choi SM, Kang MJ, Yun SH, Kwon DJ, Noh YS, Noh B** (2018) Salicylic acid-induced transcriptional reprogramming by the HAC-NPR1-TGA histone acetyltransferase complex in Arabidopsis. Nucleic Acids Res **46:** 11712–11725

**Jones JD, Dangl JL** (2006) The plant immune system. Nature **444:** 323–329

**Kachroo P, Liu H, Kachroo A** (2020) Salicylic acid: transport and long-distance immune signaling. Curr Opin Virol **42:** 53–57

**Kaufmann K, Muino JM, Osteras M, Farinelli L, Krajewski P, Angenent GC** (2010) Chromatin immunoprecipitation (ChIP) of plant transcription factors followed by sequencing (ChIP-SEQ) or hybridization to whole genome arrays (ChIP-CHIP). Nat Protoc **5:** 457–472

**Kim D, Paggi JM, Park C, Bennett C, Salzberg SL** (2019) Graph-based genome alignment and genotyping with HISAT2 and HISAT-genotype. Nat Biotechnol **37:** 907–915

**Kumar D** (2014) Salicylic acid signaling in disease resistance. Plant Sci **228:** 127–134

**Love MI, Huber W, Anders S** (2014) Moderated estimation of fold change and dispersion for RNA-seq data with DESeq2. Genome Biol **15:** 550

**Lu H** (2009) Dissection of salicylic acid-mediated defense signaling networks. Plant Signal Behav **4:** 713–717

**Malamy J, Hennig J, Klessig DF** (1992) Temperature-dependent induction of salicylic acid and its conjugates during the resistance response to tobacco mosaic virus infection. Plant Cell **4:** 359–366

**Minina EA, Bozhkov PV, Hofius D** (2014) Autophagy as initiator or executioner of cell death. Trends Plant Sci **19:** 692–697

**Mou Z, Fan W, Dong X** (2003) Inducers of plant systemic acquired resistance regulate NPR1 function through redox changes. Cell **113:** 935–944

**Nawrath C, Metraux JP** (1999) Salicylic acid induction-deficient mutants of Arabidopsis express PR-2 and PR-5 and accumulate high levels of camalexin after pathogen inoculation. Plant Cell **11:** 1393–1404

**Rekhter D, Ludke D, Ding Y, Feussner K, Zienkiewicz K, Lipka V, Wiermer M, Zhang Y, Feussner I** (2019) Isochorismate-derived biosynthesis of the plant stress hormone salicylic acid. Science **365:** 498–502

**Rivas-San Vicente M, Plasencia J** (2011) Salicylic acid beyond defence: its role in plant growth and development. J Exp Bot **62:** 3321–3338

**Serrano M, Wang B, Aryal B, Garcion C, Abou-Mansour E, Heck S, Geisler M, Mauch F, Nawrath C, Metraux JP** (2013) Export of salicylic acid from the chloroplast requires the multidrug and toxin extrusion-like transporter EDS5. Plant Physiol **162:** 1815–1821

**Spoel SH, Mou Z, Tada Y, Spivey NW, Genschik P, Dong X** (2009) Proteasome-mediated turnover of the transcription coactivator NPR1 plays dual roles in regulating plant immunity. Cell **137:** 860–872

**Sun T, Huang J, Xu Y, Verma V, Jing B, Sun Y, Ruiz Orduna A, Tian H, Huang X, Xia S, et al.** (2020) Redundant CAMTA transcription factors negatively regulate the biosynthesis of salicylic acid and N-hydroxypipecolic acid by modulating the expression of SARD1 and CBP60g. Mol Plant **13:** 144–156

**Sun T, Zhang Y, Li Y, Zhang Q, Ding Y, Zhang Y** (2015) ChIP-seq reveals broad roles of SARD1 and CBP60g in regulating plant immunity. Nat Commun **6:** 10159

**Tian T, Liu Y, Yan H, You Q, Yi X, Du Z, Xu W, Su Z** (2017) agriGO v2.0: a GO analysis toolkit for the agricultural community, 2017 update. Nucleic Acids Res **45:** W122–W129

**Tsuda K, Sato M, Glazebrook J, Cohen JD, Katagiri F** (2008) Interplay between MAMP-triggered and SA-mediated defense responses. Plant J **53:** 763–775

**van Butselaar T, Van den Ackerveken G** (2020) Salicylic acid steers the growth-immunity tradeoff. Trends Plant Sci **25:** 566–576

**Venugopal SC, Jeong RD, Mandal MK, Zhu S, Chandra-Shekara AC, Xia Y, Hersh M, Stromberg AJ, Navarre D, Kachroo A, et al.** (2009) Enhanced disease susceptibility 1 and salicylic acid act redundantly to regulate resistance gene-mediated signaling. PLoS Genet **5:** e1000545

**Wang L, Tsuda K, Truman W, Sato M, Nguyen le V, Katagiri F, Glazebrook J** (2011) CBP60g and SARD1 play partially redundant critical roles in salicylic acid signaling. Plant J **67:** 1029–1041

**Wang Y, Hu Q, Wu Z, Wang H, Han S, Jin Y, Zhou J, Zhang Z, Jiang J, Shen Y, Shi H, Yang W** (2017) HISTONE DEACETYLASE 6 represses pathogen defence responses in *Arabidopsis thaliana*. Plant Cell Environ **40:** 2972–2986

**Wildermuth MC, Dewdney J, Wu G, Ausubel FM** (2001) Isochorismate synthase is required to synthesize salicylic acid for plant defence. Nature **414:** 562–565

**Withers J, Dong X** (2017) Post-translational regulation of plant immunity. Curr Opin Plant Biol **38:** 124–132

**Zhang Y, Fan W, Kinkema M, Li X, Dong X** (1999) Interaction of NPR1 with basic leucine zipper protein transcription factors that bind sequences required for salicylic acid induction of the PR-1 gene. Proc Natl Acad Sci USA **96:** 6523–6528

**Zhou M, Lu Y, Bethke G, Harrison BT, Hatsugai N, Katagiri F, Glazebrook J** (2018) WRKY70 prevents axenic activation of plant immunity by direct repression of SARD1. New Phytol **217:** 700–712